Compact Ultra-Wideband Planar Inverted F Antenna on Laminated Paper-Based Substrate with Reduced Specific Absorption Rate

Sakshi Kumari and Vibha Rani Gupta

***Abstract*—This paper presents a laminated paper-based Planar Inverted F Antenna (PIFA) for wireless body area network (WBAN) applications. The major challenges like providing adequate thickness, uniformity of surface, and water wet ability associated with paper substrate have been transcended in this antenna design by laminating the substrate with a transparent sheet. The simulated and measured reflection coefficients of the fabricated antenna in free space and on human arm are remarkably good, validating the prototype's utility. It can operate effectively in GSM, WMTS, GPS, DCS, ISM, WiMAX, HIPERLAN, WLAN, and UWB frequency bands with S_{11} less than -10 dB and the gain ranging from 0.94 to 9.53 dB (free space) and 1.03 to 6.07 dB (on-body). The electrical size of the proposed antenna is 0.16 λg x 0.12 λg at 0.7 GHz with a group delay below 2.3 ns over the desired frequency bands. The performance characteristics are also investigated on-body and it encompasses most of the desired frequency bands for the body area network. This paper also analyses the specific absorption rate (SAR) of the designed antenna by placing it on a tissue-layered human arm model, which is 0.64 Watt/kg, complying with the SAR safety guidelines.**

***Index Terms*—Lamination, Planar Inverted F antenna, Organic material, Paper-based, Specific absorption rate, Ultra-wideband, Wireless Body Area Network.**

Original Research Paper
DOI: 10.53314/ELS2327025K

I. Introduction

The breakthrough advancements in wireless communication technology have facilitated the evolution of miniaturized and ingenious antennas for Wireless Body Area Networks (WBAN). It is a pioneering domain with applications in medical, defense, wearable computing, navigation system, etc. Various wireless frequency bandwidths are deployed for WBAN like the Medical Implant Communication System (MICS:0.4 GHz), Global System of Mobile Communication (GSM:0.85/0.9GHz), Global Positioning System (GPS:1.5GHz), Digital Communication System (DCS:1.8GHz), the Industrial Scientific Medical (ISM: 2.45GHz), Worldwide Interoperability for Microwave Access (WiMAX:3.5GHz), Wireless Body Area Network (WLAN:5.2GHz), High Performance Local Area Network (HIPERLAN: 5.8GHz), and the Ultra-Wideband (UWB:3.1-10.6GHz) [1].

Wearable antennas are utilized as a transceiver in the WBAN to transmit and receive the data between patients and physicians, as well as to transmit the patient's location. One of the most important aspects of the wearable application is the "conformability" to ease wear.

Many unconventional materials like jute [2], denim [3], cotton textile [4]-[5] shieldIt Super/Felt [6], fleece [7], leather [8], and paper [9]-[14] are utilized for realizing antennas for WBAN applications. The unconventional and conformal substrate, paper, has many features like low cost, low surface profile, flexibility, eco-friendly, organic, and biodegradability, making it an excellent candidate for wearable applications. Due to its properties, the paper has been extensively exploited in a wide range of applications like energy storage, environmental monitoring, food quality monitoring, and diagnosis [9].

Paper-based antennas have been reported with different configurations such as CPW fed monopole for GPS [10], WLAN [11], star-shaped patch with two *L* stubs [12], monopole with U slot for triband GPS/WiMAX, WLAN, and HiperLan/2 bands [13]. In addition, the monopole configuration of patch antenna with an ultra-wideband characteristic (2.2–10 GHz) is reported in [14] which does not include the lower frequency bands. Most paper-based antennas reported in the literature are of monopole arrangement and are designed for specific applications.

Considering the issue of SAR, the microstrip patch configuration is one of the best configurations in terms of conformability, being less thick, and low SAR due to the ground plane [15]. However, the microstrip patch antenna has its limitation due to narrow bandwidth. In [16], a wideband rectangular patch (2.45 – 6 GHz) is reported, but it does not incorporate all the frequency bands of WBAN.

Therefore, PIFA is chosen as the antenna configuration, having a ground plane under the complete radiating patch. The bandwidth enhancement of PIFA, starting from the lower frequency band till UWB, is a critical issue, as well as its reduction in size for body area communications. Some of the techniques described in the literature for increasing the antenna bandwidth and reducing its size include stub loading; capacitive, inductive loading of the top plate; meandering ground plane with slots [17]; the use of different shapes of feed plate like square, rectangular, U, triangular [18]; dielectric loading [19]; the introduction of slots [20]; and modifying the shorting pin location [21].

Manuscript received 20th October 2022. Received in revised form 1st March 2023, and 2nd April 2023. Accepted for Publication 19th April 2023.

Sakshi Kumari is with the Department of Electronics and Communication Engineering, Birla Institute of Technology, Mesra, Jharkhand, India. (Corresponding author e-mail: sakshi501@gmail.com)

Vibha Rani Gupta is with the Department of Electronics and Communication Engineering, Birla Institute of Technology, Mesra, Jharkhand, India (email: vrgupta@bitmesra.ac.in)

Apart from its advantages, the paper-based substrate has one of the most significant drawbacks of being hydrophilic, which degrades the performance characteristics of the designed antenna over time due to the absorption of atmospheric humidity.

There have been various research endeavors in the past to acknowledge the conformal issues in antenna design. However, very few researchers have addressed the limitations of the hydrophilic nature of printed antennas on textile or paper-based substrates. Some of the reported techniques for textiles are coating with waterproof materials such as PVC, silicone, or acrylic [22]-[23]. Kim et al. [24] proposed the method of coating paper-based antennas with parylene coating to prevent rusting and degradation of antenna performance as the entire metallic part is not exposed to atmospheric humidity. According to the authors [24], the wet silicone coating is incompatible with hydrophobic materials. It can induce mechanical stress during or after the procedure, and acrylic coating is resilient to harsh environmental conditions and abrasions. In [25], four different types of coating, parylene C, dielectric paste, silicone spray, and PET film, were applied on Gore-Tex fabric with textile plastic on both sides to protect the patch antenna surface. Thielens et al. [26] developed spray-coated antennas on PEN and Polyimide Kapton (plastic material) using optimized silver nanoparticles water-solvent based ink. This method is an alternative to screen and inkjet printing of antennas which are not only an expensive method but there are also chances of spreading ink. A resin-coated photo paper is utilized to develop a conformal multiband monopole antenna in [27] for handheld and wearable devices.

This paper introduces a novel technique of laminating paper with a transparent sheet to mitigate the problem of performance degradation due to ambient humidity of the environment and prolong the lifetime of paper-based electronics. The antenna printed on the paper-based substrate, laminated with a transparent sheet, not only overcomes the limitations of paper-based antennas without deteriorating the free space and on-body performance characteristics but also replaces the tedious job of coating antennas with any waterproof coating.

In recent research, none of the papers has been accounted for, which includes all the referenced frequency bands for WBAN application based on the laminated paper-based substrate.

The proposed antenna is an ultra-wideband PIFA with a wide frequency bandwidth of 10.28 GHz (0.75 GHz to 11.03 GHz) at -10 dB using the laminated paper-based substrate for the body area network. F-shaped and annular ring-shaped slots are incorporated into the radiating patch to reduce the size, whereas the feed is modified to achieve impedance matching. This single antenna can be extensively utilized for data transfer to physicians, communication between equipment, sports monitoring, identification of location, tracking, and voice communication.

Section II discusses the material characterization for antenna design. The design approach taken to arrive at the final proposed antenna geometry is explained in section III. The result and discussions are presented in section IV. A comparison of the proposed antenna with other paper-based ultra-wideband antennas is discussed in section V. Finally, in section VI, the conclusions are stated.

II. Dielectric Characterization Of Substrate

The paper and transparent sheets offered in the shop differ in quality, texture, thickness, and density; hence, their relative permittivity and loss tangent also differ. Consequently, the material characterization of laminated paper-based substrates is an essential step before its use in antenna design.

There are several methods that have been reported in the past for dielectric characterization, such as T Resonator, Ring Resonator, Resonant method, Transmission Line, and Cavity Perturbation method [28]. The two methods considered for the paper substrate and transparent sheet characterization are the Transmission Line and Cavity Perturbation methods [15, 28]. The substrate is prepared by stacking four sheets of paper and then laminated by a transparent film sheet to obtain adequate thickness. The calculated values of dielectric characterization are approximately the same and verified [15], as enumerated in Table I.

TABLE I
Dielectric Constant and Loss Tangent of Paper and Transparent Sheet

Method	Paper		Transparent sheet	
	Dielectric Constant	Loss Tangent	Dielectric Constant	Loss Tangent
Transmission Line	2.8	0.0349	2.4	0.0181
Cavity Perturbation	2.82	0.035	2.45	0.018

III. Design Approach For Geometry Of Proposed Antenna

The proposed miniaturized ultra-wideband PIFA on a laminated paper-based substrate is an extension of the designed antenna [29], based on the initial design equation.

$$L_p + W_p - W_{sh} = \lambda_0/4 \tag{1}$$

where, λ_0 is the operating wavelength, L_p is the patch length, W_p is the patch width and W_{sh} is the width of shorting strip.

In this research paper, a laminated paper-based substrate with reduced dimensions is used for the design. The reduced size of radiating patch and substrate are 32 x 42 x 0.3 mm^3 and 48 x 42 x 1.6 mm^3, respectively. The design approach to reach the final structure is represented in Fig. 1. Fig. 2 depicts the simulated S_{11} response for the step-by-step approach followed to reach the final proposed antenna. An effort has been made to minimize the antenna's size after the several steps shown in Fig. 1.

Step 1 is the design of an ultra-wideband PIFA on a laminated paper-based substrate of size 48 x 42 x 1.6 mm^3, depicted in Fig. 1(a). This design covers frequencies ranging from 1.38 GHz to 14.85 GHz at -6 dB of S_{11}. At height H, a rectangular

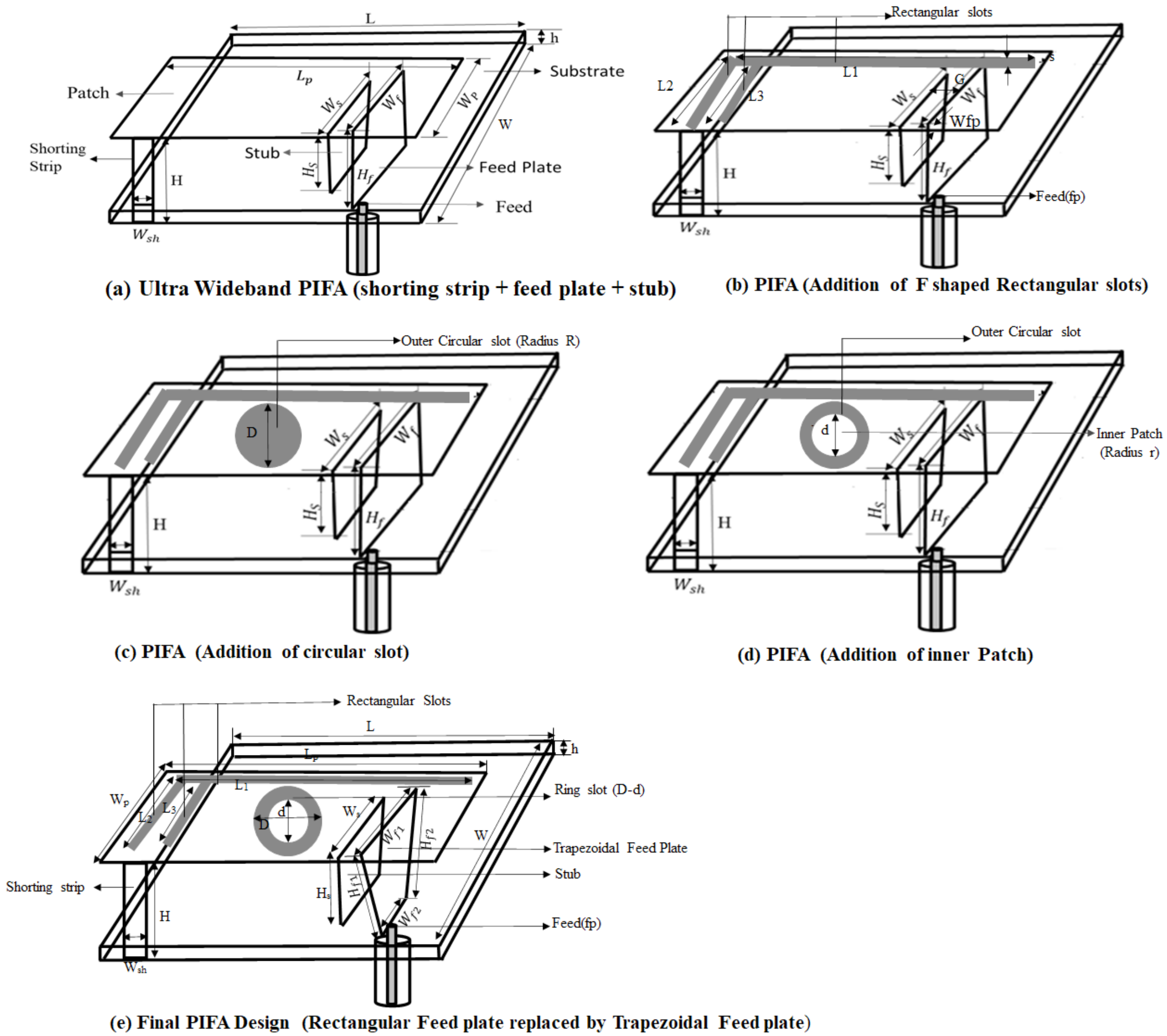

Fig. 1. Design approach of proposed miniaturized PIFA.

patch of L_p x $W_p \times t$ is placed above the substrate of dimension L x W x h. The space between the substrate and patch is filled with styrofoam having a dielectric constant of 1.11. A shorting plate/strip ($W_{sh} \times H$ x t) instead of shorting pin is used to shorten the antenna. A feed plate technique is used to feed the antenna. A rectangle shaped plate with dimensions $W_f \times H_f \times t$ which is connected with a coaxial probe is used for feeding. The inner conductor of the probe is connected to the feeding plate, while the outer conductor of the probe is connected to the ground. For impedance matching, a stub (W_s x H_s x t) is also utilized. The separation between the feed plate and stub is denoted by 'G'. Parametric studies have been carried out to optimize the width of the feed plate, shorting plate, and G to obtain maximum impedance bandwidth. In step 2, three rectangular slots (L_1, L_2, and L_3), shown in Fig. 1(b) are added, which act as a slow wave structure and shift the first resonant frequency to 0.64 GHz. The aggregate length of slots L_S (L_1+ L_2+ L_3) is decided through the parametric study. The antenna spans the frequency band 0.35–15 GHz at S_{11} of -6 dB, except for the frequency band 12.04 –12.34 GHz.

The rectangular feed plate width (W_f) is optimized in the third step of the parametric study. The optimal length of the feed plate is 21 mm, at 1 mm (W_{fp}) from the radiating patch. The feed position is fixed at (fp)7 mm from the feed plate's edge. The optimized reflection coefficient versus frequency is displayed in step 3 of Fig. 2. The optimized dimensions and the feed plate's position enhance the impedance matching at high frequency, covering the entire frequency spectrum 0.35–14.35 GHz at -6 dB of S_{11} while it is 12.65 GHz (0.35 GHz to 13.00 GHz) at S_{11}= -10 dB, excluding 4.34 –4.86 GHz.

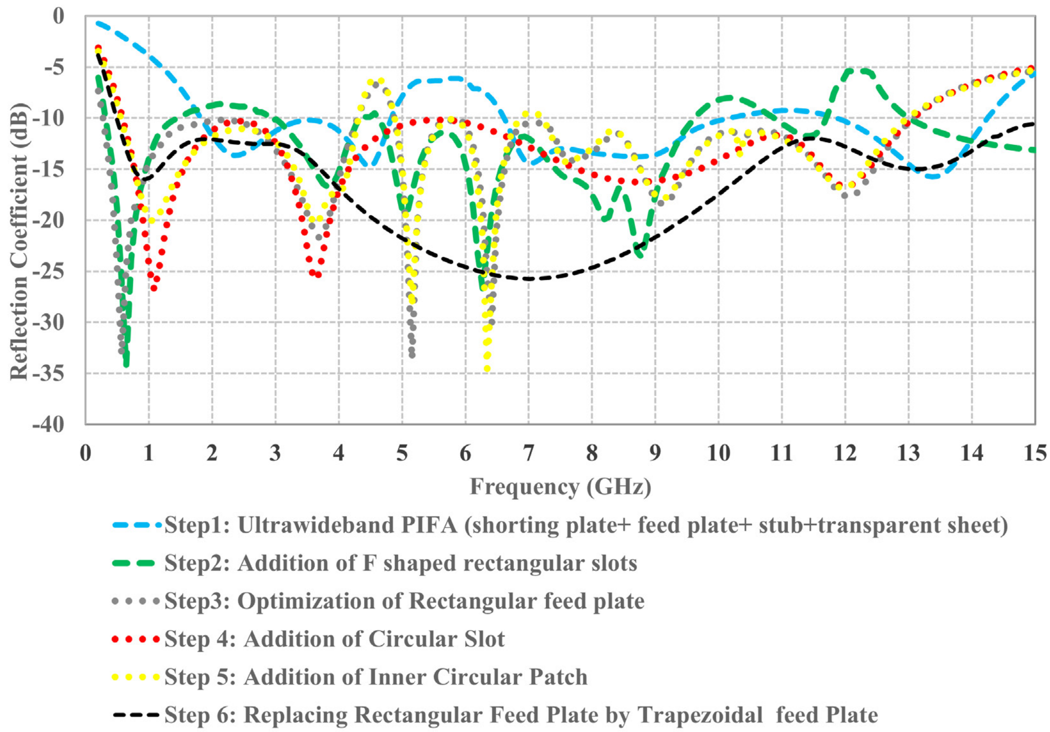

Fig. 2. Comparison of reflection coefficient of different steps to reach the proposed antenna.

In the fourth stage, a circular slot of radius (D) 6 mm (Fig. 1(c)) is incorporated to minimize the area of the radiating patch to 26.09% but slightly shifts the frequency band. Its reflection coefficient response is shown in step 4 of Fig. 2. The frequency range covered in this case is from 0.64 GHz to 13.08 GHz at -10 dB reference.

In the next step, a circular patch (d) is added in the circular slot in the radiating patch to transform it into a ring slot (Fig. 1(d)) with its reflection coefficient depicted in step 5 of Fig. 2. This gives almost the similar reflection coefficient response as obtained in step 3 with an improvement in S_{11} in the frequency band of 1.75–2.57 GHz. But still, the frequencies between 4.34 – 4.86 GHz were not covered.

As seen from Fig. 1(a-d), a rectangle-shaped plate with dimensions $W_f \times H_f \times t$ is initially used for feeding. Finally, in the proposed structure (last step), the shape of the feed plate is changed from a rectangular to a trapezoidal shape, as depicted in Fig. 1(e), which improves impedance matching over the entire range of the desired frequency band. At the center frequency of 7.25 GHz, the input impedance is 82.56-j14 Ω and 50.06-j3Ω with rectangular and trapezoidal feed plates, respectively. As the bandwidth of an antenna is affected by the impedance matching and the quality factor [30], the impedance bandwidth of the proposed antenna increases by 17.31% due to the trapezoidal feed plate.

In the parametric study for the feed position on the trapezoidal feed plate, stub related parameters like stub position, height, width, and the gap between the stub and feed plate (G) are also analyzed for the proposed antenna's final design. The final schematic of the proposed antenna is depicted in Fig. 1(e). The frequency band of 0.49–15 GHz is covered at $S_{11} \leq$ -10 dB for the final geometry as depicted in Fig. 1(e) and optimized dimensions reported in Table II.

TABLE II
DETAILED DIMENSIONS OF PROPOSED ANTENNA

Parameter	Dimension (mm)	Parameter	Dimension (mm)
L	42	L3	24
W	48	W_{f1}	21
h	1.6	W_{f2}	7
L_p	42	H_{f1}	8.04
W_p	32	H_{f2}	10.9
t	0.3	W_{sh}	3
W_s	4.8	H	7.9
Hs	6	D	6
L1	36.5	d	5
L2	28.2	Ls(L1+L2+L3)	88.7

IV. RESULT AND DISCUSSIONS

An antenna designed for a body area network can be placed on different body parts like the arm, forearm, chest, thigh, wrist, etc. But putting the antenna on the arm is more suitable as it does not obstruct day-to-day human activities. The human arm is designed in HFSS[31] to evaluate the antenna characteristics near the human arm by considering the dielectric characteristics of skin, fat, muscle, and bone at various frequencies [32]. It also determines how an antenna interacts with the body part. The fabricated prototype is displayed in Fig. 3.

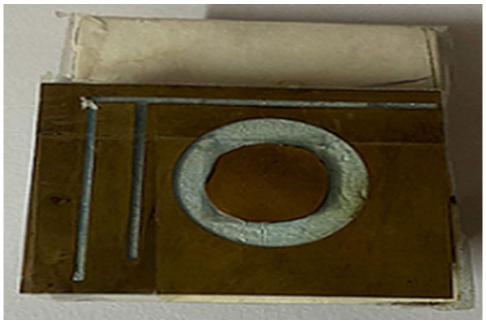

Fig. 3. Fabricated prototype

A. Reflection Coefficient

A representation of the simulation and measurement of free-space reflection coefficients is illustrated in Fig. 4. The graph illustrates that the simulated bandwidth in free space is 0.49 –15 GHz. However, the measured bandwidth is only 10.04 GHz, covering frequencies between 0.71–10.75 GHz, comprising all the important WBAN bands.

The discrepancy in simulated and measured S_{11} may be credited to the misalignment of the stub, feed plate, shorting plate, and feed pin in the fabricated antenna. Also, the dielectric constant was verified at 2.45 GHz and the same was used in the simulation over the wide frequency band. But the dielectric constant and loss tangent varies over the frequency range, which may affect the measured results.

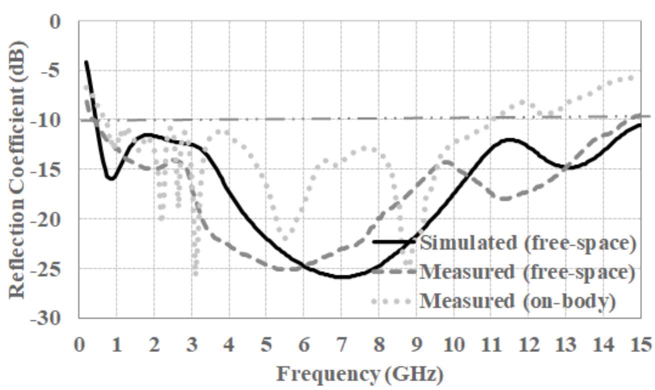

Fig. 4. Reflection coefficient of proposed antenna in free-space and on-body (arm).

As shown in Fig. 4, the on-body (arm) measured reflection coefficient is 10.28 GHz, over the frequency range of 0.75 GHz – 11.03 GHz. A slight shift in on-body S_{11} characteristics is observed due to the dielectric characteristics of body tissues, but it incorporates all the desired frequency bandwidths for WBAN applications.

B . Gain

The free-space and on-body gain at desired frequencies are obtained through simulations and verified by measurement, as shown in Fig. 5. The measured peak gains at center frequencies of desired frequency bands lie in the range of 0.94 to 9.53 dB in free-space and 1.03 dB to 6.07 dB for on-body.

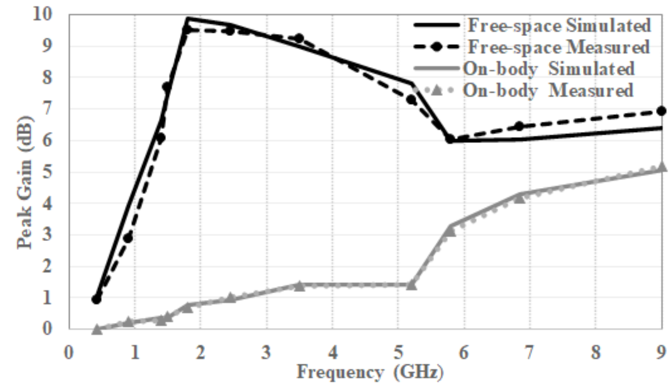

Fig. 5. Simulated and measured peak gain.

C. Group Delay

For a UWB antenna, group delay is a significant performance characteristic [33]. The two identical proposed antennas in the far field region are arranged in the front-to-front orientation.

Two different set-ups were considered for its determination. In the first arrangement, both the transmitting and receiving antennas are mounted in the free space. The group delay variance is between 0.01 ns and 2.25 ns for the specified frequency ranges. In the second case, it lies between 0.01 ns and 1.70 ns, for the transmitter mounted on the human arm and the receiver located in the free space at 0.6 m.

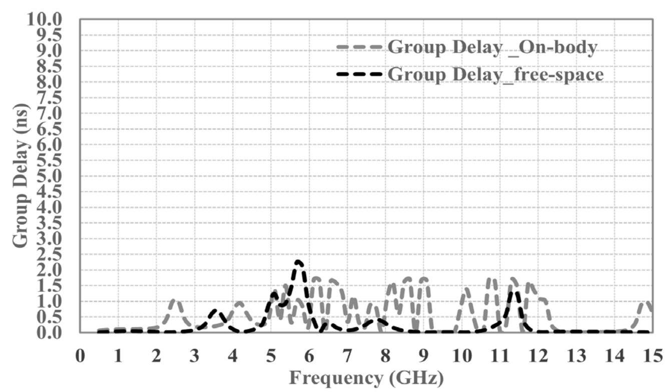

Fig. 6. Group delay response.

Fig. 6 displays the simulated group delay responses, which shows good phase linearity for short-range communication and high data rate applications.

D. Radiation Pattern

Fig. 7 shows the normalized E-plane and H-plane simulated on-body radiation pattern at the center frequencies of desired frequency bands. Because of the measurement limitations, the radiation pattern was not measured on the human arm.

E. Specific Absorption Rate

An essential consideration while developing an antenna for WBAN is SAR. The proposed antenna is placed 2 mm away from the modeled human arm [31] to estimate SAR in close proximity to the human body, as shown in Fig. 8. The human

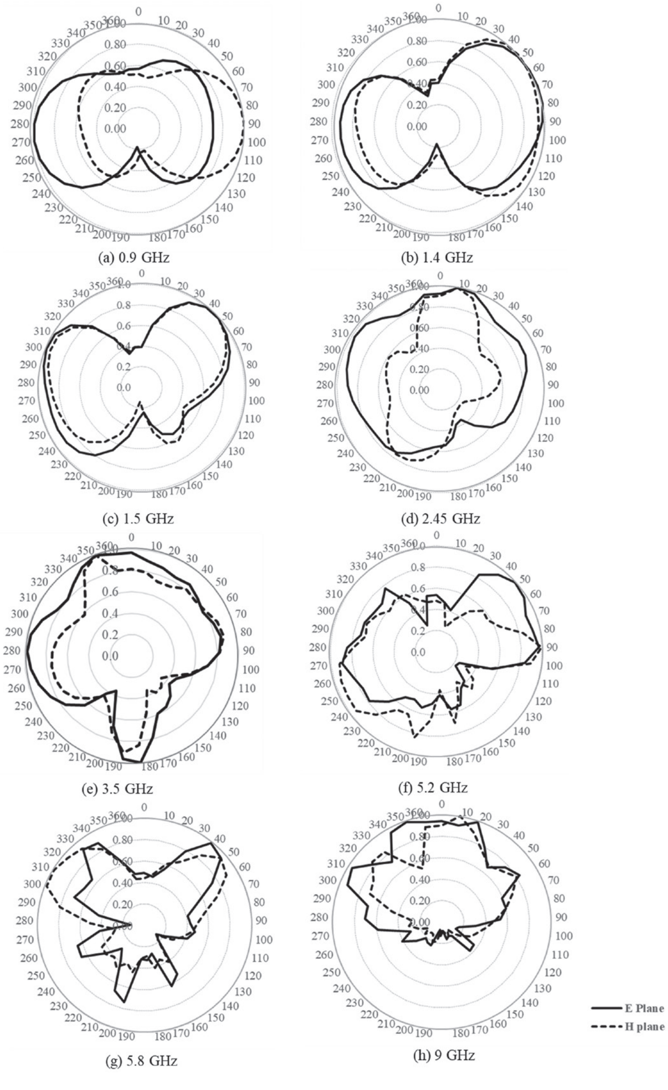

Fig. 7. Simulated on-body radiation patterns.

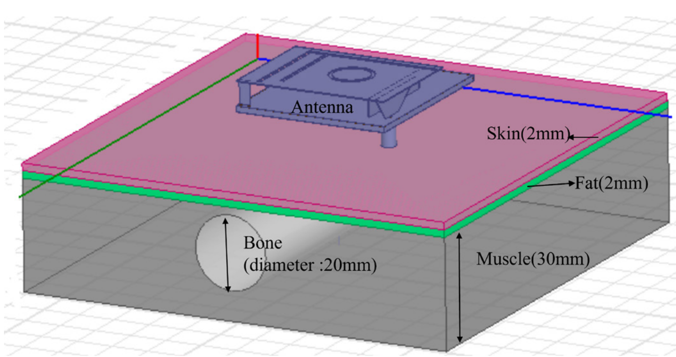

Fig. 8. Placement of antenna on modeled human arm for SAR evaluation**.**

arm is modeled at all desired frequencies (0.4 GHz, 0.9 GHz, 1.5 GHz, 1.8 GHz, 2.45 GHz, 3.5 GHz, 5.2 GHz, and 5.8 GHz), one at a time. Consequently, SAR at all desired frequencies is obtained through simulation.

The simulated SAR field distribution is depicted in Fig. 9. The SAR varies between 0.023–0.64 Watt/kg, which is quite below the limits specified by ICNIRP safety guidelines [34]. Hence the designed antenna is amenable for use in WBAN.

V Comparison Of THE Proposed Antenna With Other Paper-Based Ultrawideband Antennas

The proposed antenna is compared to some of the most recent paper-based antennas in terms of antenna topology, the permittivity of the substrate, electrical patch size, presence/ absence of ground plane, gain, and bandwidth. There are many application-specific antennas designed on Paper-based substrates available in the literature. However, only the wideband antennas are considered here for comparison with the proposed antenna, as depicted in Table III.

Table III indicates that most of the researchers chose a monopole configuration to realize the UWB paper-based antenna, which can even result in a considerably wider bandwidth [37-39]. But, very few authors have reported SAR for paper based UWB antennas [29,40-41]. The existence of an incomplete ground plane of monopole configuration degrades the SAR of the designed antenna, mainly when used at a lower frequency range for WBAN applications [31].

As compared to [29], the electrical size of the proposed antenna is reduced by 47.82%. In addition, as a contrast to a paper substrate, the substrate used in this work is a laminated paper-based substrate.

Thus, the novelty of this designed antenna is an achievement of ultra-wide bandwidth of 10.04 GHz (off-body) and 10.28 GHz (on-body) at S_{11} < -10 dB on a laminated paper-based substrate with a complete ground plane. Also, the antenna's size is 0.16 λg x 0.12 λg at a lower frequency of 0.7 GHz, which is comparatively much smaller. For the very first time, a transparent sheet is used to laminate a paper-based antenna to mitigate its limitations.

VI. Conclusion

A compact ultra-wideband PIFA with a bandwidth of 10.04 GHz (0.71 GHz –10.75 GHz) in free- space and 10.28 GHz (0.75 GHz –11.03 GHz) for on-body at S_{11} < -10 dB is proposed. A laminated paper-based substrate is used for the first time to overcome the limitations of the paper substrate.

The antenna covers all the desired bands of frequencies essential for body area networks (GSM(0.88–0.96 GHz), WMTS(1.395–1.40 GHz), GPS(1.565–1.585 GHz) DCS(1.710–1.88 GHz), PCS(1.85–1.990 GHz), UMTS(1.92–2.17 GHz), ISM(2.4–2.48 GHz), WiMAX (3.3–3.8 GHz), HiperLAN/2 (5.15–5.35 GHz), WLAN (5.725–5.85 GHz) and a UWB band (3.1–10.6 GHz)). The measured specific absorption rate is 0.64 Watt/kg, much below the SAR radiation safety guidelines. The designed antenna has a group delay lesser than 2.3 ns which indicates better phase linearity and the maximum measured peak gain of 9.53 dB (free space) and 6.07 dB (on-body). Thus, the proposed antenna is ideal for a wireless body area network as it can serve multiple applications.

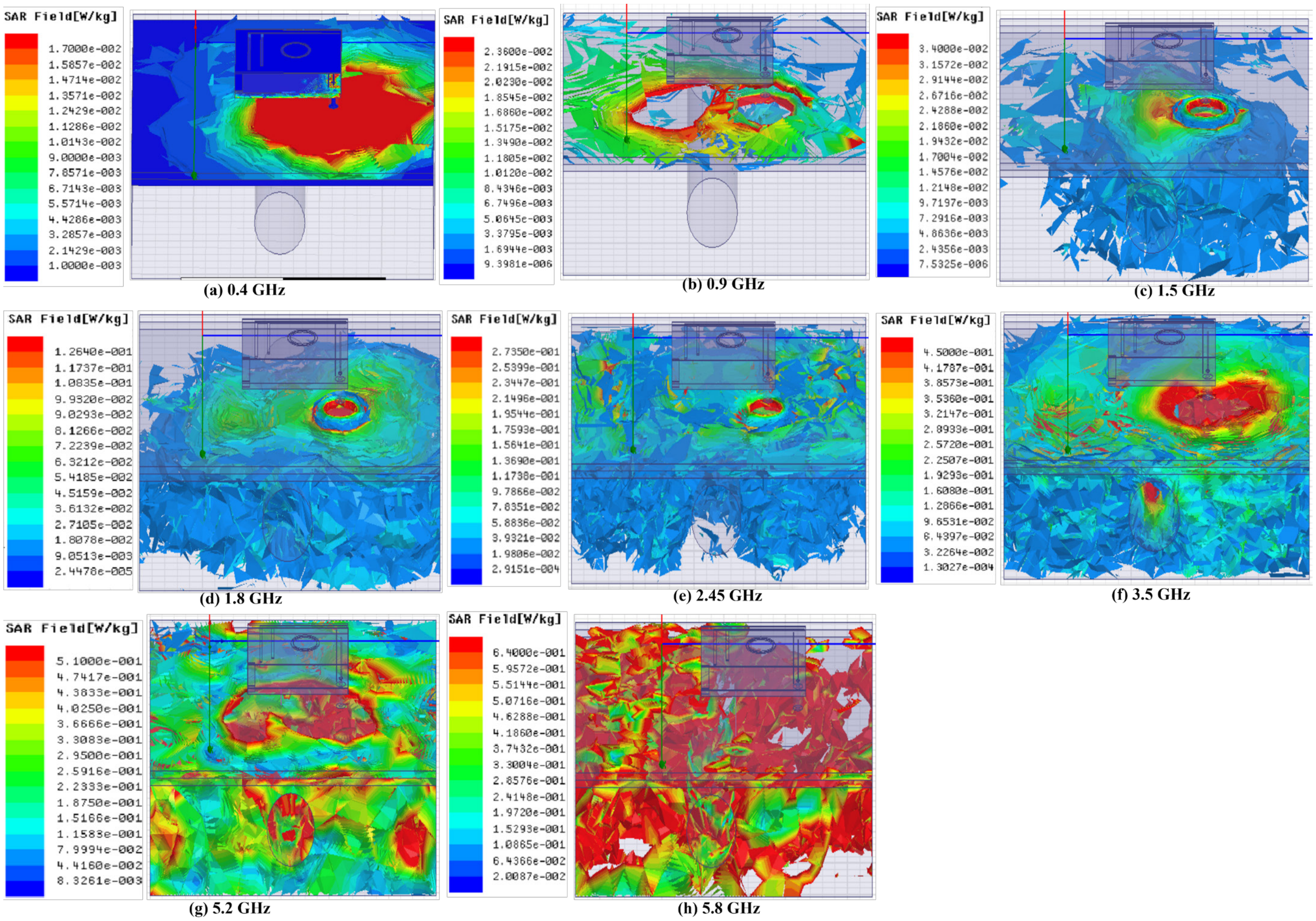

Fig. 9. SAR field distribution at the center frequencies of the desired band.

TABLE III
COMPARISON OF PROPOSED ANTENNA WITH OTHER PAPER-BASED UWB ANTENNAS

Ref/year	Antenna Type	Substrate Used (ε_r)	Patch Size (λg x λg)	Ground plane	Max. Peak gain (dB)	Max. SAR (Watt/kg)	Operating Frequency Band
[14]2017	Monopole	Paper (3.184)	0.65 x 0.36	Partial	1.52(free-space)	-	2.2 to 10 GHz
[27]2015	Monopole	Resin-coated photo-paper(3.2)	0.35 x 0.40	Partial	Approx :0.5 (1.71-3.03GHz) Approx:3 (4.51–5.5 GHz)	-	1.71–3.03 GHz 3.37–3.66 GHz 4.51–5.5 GHz
[29]2019	PIFA	Paper based(2.82)	0.23 x 0.16	Full	11.55(freespace)	0.69	0.7 to 11.3 GHz free-space
[35]2012	(i)Fractal Monopole (ii)Koch-Sierpinski	Paper (3)	(i)0.60 x0.26 (ii)0.35x0.58	Partial	2.8	-	3.5 to 10 GHz 2 to 5.5 GHz
[36]2012	Vivaldi	Paper (3.05)	0.92 x 1.1	Partial	8	-	2 to 10 GHz
[37]2018	Monopole	Kodak photo paper (2.85)	0.60 x 0.60	Partial	4.87 (avg)	-	3.2 to 30 GHz
[38]2020	Monopole	PET paper(3.2)	0.33 x 0.24	Partial	4.91(avg)	-	1.66 to 56.1GHz
[39]2021	Monopole	PET paper (3.2)	0.85 x 0.45	Partial	3.94 (avg)	-	3.04 to 10.7 GHz 15.18 to 18 GHz
[40]2021	Monopole	Photopaper(3.2)	0.39 x 0.56	Partial	1.61	1.99	2.36- 2.40 GHz 2.40- 2.48 GHz
[41]2022	Hexagonal	Photopaper(3.2)	0.41 x 0.54	Partial	3.48	1.93	2.30-5.30 GHz
Proposed Antenna	PIFA	Laminated Paper (Paper:2.82 Transparent sheet:2.45)	0.16 x 0.12	Full	9.53 (freespace) 6.07(on-body)	0.64	0.71 to 10.75GHz: free-space 0.75 to 11.03GHz on-body

References

[1] K. Hasan, K. Biswas, K. Ahmed, N. S. Nafi, and Md. S. Islam, "A comprehensive review of wireless body area network," *J. Netw. and Comput. Appl.*, vol. 143, pp.178-198, July 2019.

[2] K. Zeouga, L. Osman, A. Gharsallah, and B. Gupta, "Truncated patch antenna on jute textile for wireless power transmission at 2.45 GHz," *Int. J. Adv. Comput. Sci. Appl*., vol. 9, no. 1, pp. 301-305, 2018. doi: 10.14569/IJACSA.2018.090141.

[3] M. I. Ahmed, M. F. Ahmed, and A. -El. A. Shaalan, "Novel electro textile patch antenna on jeans substrate for wearable applications," *Prog. Electromagn. Res. C*, vol. 83, pp.255–265, April 2018.

[4] S. M. H. Varkiani and M. Afsahi, "Compact and ultra-wideband CPW-fed square slot antenna for wearable applications," *AEU Int. J. Electron. Commun.* , vol. 106, pp.108–115, 2019.

[5] A. Anbalagan, *et al*., "Realization and analysis of a novel low-profile embroidered textile antenna for real-time pulse monitoring," *IETE J. Research*, vol.68, pp.4142-4149, 2022. doi: 10.1080/03772063.2020.1787877

[6] F. R. Kareem, M. El. Atrash, A. A. Ibrahim, M. A. Abdalla, "All-textile inspired-folded dipole antennas for on/off-body communications medical applications," *Alexandria Engg. J.*, vol. 61, no. 11, pp. 8751-8761, Feb. 2022.

[7] N. S. M. Yaziz, and M. K. A. Rahim, "Wideband textile antenna for wearable application," *in Proc. 2015 IEEE Int. RF and Microw. Conf*., Malaysia, December 14 - 16, 2015, pp.132-135.

[8] M. S. Mahmud, F. Jinan, J. Jabri, and B. Mahjabeen, "Compact UWB wearable antenna on leather material for wireless applications", *in Proc. 2013 IEEE Antennas and Propag. Society Int. Symposium*, Orlando, FL, USA, 2013, pp. 2191-2192.

[9] K. Punpattanakul, *et al.*, "A novel patterning method for three-dimensional paper-based devices by using inkjet-printed water mask," *Cellulose*, vol. 25, pp.2659–2665, Feb.2018.

[10] A. M. Mansour, N. Shehata, B. M. Hamza, and M. R. M. Rizk, "Efficient design of flexible and low-cost paper-based inkjet-printed antenna," *Int. J. Antennas Propag*., vol. 2015, Article ID 845042, pp.1-6, 2015.

[11] F. L. Wignes, C. Glascoe, G. Makar, T. Karakolak, and P. Sekhar, "A paper based 2-element antenna for WLAN MIMO applications fabricated using inkjet technology," *Microw. Opt. Technol. Lett.,* vol. 59, pp.2785–2790, Aug. 2017.

[12] W. N. N. W. Marzudi, Z. Z. Abidin, S. H. Dahlan, K. N. Ramli, and M. R. Kamarudin, "Performance of star patch antenna on a paper-based substrate material," *ARPN J. Eng. Appl. Sci*., vol.10, no. 19, pp. 8606-8612,Oct. 2015.

[13] H. F. Abutarboush, and A. Shamim, "Paper-based inkjet-printed tri-band U-slot monopole antenna for wireless applications," *IEEE Antennas Wireless Propag. Lett*., vol. 11, pp.1234-1237, 2012.

[14] H. P. Phan, T. P. Vuong, P. Benech, P. Xavier, P. Borel, and A. Delattre, "Low-cost wideband antenna on paper substrate", *in Proc. 2017 11th European Conference on Antennas and Propagatio*n, France, 2017, pp. 2168-2171.

[15] S. Kumari and V. R. Gupta, "Characterization of laminated paper-based substrate for the ISM band antenna design", *Lecture Notes in Engineering and Computer Science: Proc. of The World Congress on Engineering and Computer Science 2019*, Oct. 2019, San Francisco, USA, pp124-128.

[16] D. S. Marotkar, and P. L. Zade, "Microstrip antenna with photographic paper substrate for WLAN," *Int. J. Inf. and Commun. Technol*., vol. 7, no. 2, pp.67-70, Aug. 2018.

[17] A. Verma and G. Saini, "Different size reduction techniques of PIFA antenna: A review," *ICRTED*, vol.1 spl. Iss. 2, pp.126-128, May 2014.

[18] R. Feick, H. Carrasco, M. Olmos, and H. D. Hristov, "PIFA input bandwidth enhancement by changing feed plate silhouette," *Electron. Lett*., vol.40, no.15, July 2004.

[19] Y. Hwang, Y. P. Zhang, G. X. Zheng, and T. K. C. Lo, "Planar Inverted F antenna loaded with High Permittivity Material", *Electron. Lett*., vol. 31, no. 20, pp.1710–1712, Sept.1995. doi: 10.1049/el:19951184.

[20] K. L. Wong, and K. P. Yang, "Modified planar inverted F antenna," *Electronics Lett.*, vol. 34, no. 1, pp.7–8, Jan. 1998. doi:10.1049/EL:19980102

[21] Y. J. Wang, C. K. Lee, W. J. Koh, and Y. B. Gan, "Design of small and broad-band internal antennas for IMT-2000 mobile handsets", *IEEE Trans. Microw. Theory Techn*., vol. 49, no. 8, pp.1398–1403, Aug.2001 doi: 10.1109/22.939919.

[22] A. Tsolis, W. G. Whittow, A. A. Alexandridis, and J. Y. C. Vardaxoglou, "Embroidery and related manufacturing techniques for wearable antennas: challenges and opportunities," *MDPI, Electron*., vol.3, no.2, pp. 314-338, May 2014.

[23] S. B. Roshni, M. P. Jayakrishnan, P. Mohanan, and K. P. Surendran, "Design and fabrication of an E-shaped wearable textile antenna on PVB-coated hydrophobic polyester fabric," *Smart Mater. Struct*., vol. 26, no.10 pp.1-8, Sept. 2017.

[24] S. Kim and M. M. Tentzeris, "Parylene coated waterproof washable inkjet-printed dual-band antenna on paper substrate," *Int. J. Microw. Wireless Technol.*, vol. 7, no. 2, pp. 814-818, 2018.

[25] J. J. Heikkinen, T. T. Laine-Ma, and M. A. Kivikoski, "Flexible fabric-base patch antenna with protective coating," *2007 IEEE Antennas and Propag. Society Int. Symposium*, Honolulu, HI, USA, June 2007, pp. 4168-4171, doi: 10.1109/APS.2007.4396459.

[26] A. Thielens, I. Deckman, R. Aminzadeh, A. C. Arias, and J. M. Rabaey, "Fabrication and characterization of flexible spray-coated antennas," *IEEE Access*, vol. 6, pp. 62050-62061, Nov 2018.

[27] H. F. Abutarboush, M. F. Farooqui, A. Shamim, "Inkjet-Printed wideband antenna on resin-coated paper substrate for curved wireless devices," *IEEE Antennas Wireless Propag. Lett.*, vol. 15, pp. 20-23, 2016.

[28] L. F. Chen, C. K. Ong, C. P. Neo, V. V. Varadan and V. K. Varadan, "*Microwave Electronics Measurement and Materials Characterization*," John Wiley & Sons, 2004. ISBN: 0-470-84492-2.

[29] S. Kumari, and V. R. Gupta, "Super ultrawideband planar inverted F antenna on paper based substrate with low SAR," *ECTI Trans. Electr. Eng. Electron. Commun*., vol. 17, no.2, pp.204-213, Aug. 2019.

[30] C. A. Balanis, "*Antenna Theory: Analysis and Design*," 3rd ed., John Wiley & Sons, 2005. Ch. 14. ISBN: 0-471-66782-X.

[31] S. Kumari and V. R. Gupta, "Measurement of specific absorption rate of monopole patch antenna on human arm," *Int. J. of Microw. and Opti. Technol.,* vol.10, no.3, pp.190-194, May 2015.

[32] Calculation of the Dielectric Properties of Body Tissues in the frequency range 10 Hz – 100 GHz, Italian National Research Council, Institute of Applied Physics. Available: http://niremf.ifac.cnr.it/tissprop/htmlclie/htmlclie.php

[33] P. McEvoy, M. John, S. Curto, and M. J Ammann, "Group delay performance of ultra-wideband monopole antennas for communication applications," *in Proc. 2008 Loughborough Antennas and Propag. Conf*., Loughborough, March 2008, pp. 377-380.

[34] International Commission on Non-Ionizing Radiation Protection (ICNIRP). "Guidelines for limiting exposure to electromagnetic fields (100 kHz to 300 GHz)." *Health physics 118.5*, pp. 483-524, 2020

[35] A. R. Maza, B. Cook, G. Jabbour, and A. Shamim, "Paper-based inkjet-printed ultra-wideband fractal antennas," *IET Microw. Antennas Propag*. vol. 6, iss. 12, pp.1366–1373, 2012.

[36] B. S. Cook, and A. Shamim, "Inkjet printing of novel wideband and high gain antennas on low-cost paper substrate," *IEEE Trans. Antenna Propag*., vol. 60, no. 9, pp. 4148-4156, 2012.

[37] T. K. Saha, T. N. Knaus, A. Khosla, and P. K. Sekhar, "A CPW-fed flexible UWB antenna for IoT applications," *Microsyst. Technol.*, vol.28, pp.5–11, Dec. 2018.

[38] Md. R. Hasan, M. A. Md., Riheen, P. Sekhar, and T. Karacolak, "Compact CPW-fed circular patch flexible antenna for super-wideband application," *IET Microw., Antennas Propag.*, vol. 14, iss. 10, pp. 1069-1073, May 2020.

[39] S. G. Kirtania, B. A. Younes, A. R. Hossain, T. Karacolak and P. K. Sekhar, "CPW-Fed Flexible Ultra-Wideband Antenna for IoT Applications," *Micromachines MDPI*, vol. 12, no. 453, pp.1-13, April 2021.

[40] A. Jabbar, A. Arif, M. Zubair, K. Riaz, and M. Q. Mehmood, "A Low-cost Photopaper Based Wideband Wearable Antenna for WBAN Applications," in *Proc. 2021 18th International Bhurban Conference on Applied Sciences. and Technologies (IBCAST)*, Islamabad, Pakistan, Jan. 2021, pp. 942-945.

[41] A. Jabbar, M. Zubair, M. A. Naveed, M. Q. Mehmood, and Y. Massoud, "A photopaper-based low-cost, wideband wearable antenna for wireless body area network applications," *IET Microw. Antennas Propag*., vol.16, pp.962–970, 2022.